AIP Journal of Applied Physics

Experimental and simulation analysis of concave-down resistance curve during electromigration in solder joints

C. K. Lin, Yuan Wei Chang, and Chih Chen

Citation: Journal of Applied Physics **115**, 083707 (2014); doi: 10.1063/1.4867048
View online: http://dx.doi.org/10.1063/1.4867048
View Table of Contents: http://scitation.aip.org/content/aip/journal/jap/115/8?ver=pdfcov
Published by the AIP Publishing

Articles you may be interested in

Electromigration induced Kirkendall void growth in Sn-3.5Ag/Cu solder joints
J. Appl. Phys. **115**, 083708 (2014); 10.1063/1.4867115

Influence of Cu column under-bump-metallizations on current crowding and Joule heating effects of electromigration in flip-chip solder joints
J. Appl. Phys. **111**, 043705 (2012); 10.1063/1.3682484

Electromigration effect on pancake type void propagation near the interface of bulk solder and intermetallic compound
J. Appl. Phys. **105**, 063710 (2009); 10.1063/1.3088946

Effect of contact metallization on electromigration reliability of Pb-free solder joints
J. Appl. Phys. **99**, 094906 (2006); 10.1063/1.2193037

Electromigration in Pb-free flip chip solder joints on flexible substrates
J. Appl. Phys. **99**, 023520 (2006); 10.1063/1.2163982

[This article is copyrighted as indicated in the article. Reuse of AIP content is subject to the terms at: http://scitation.aip.org/termsconditions. Downloaded to] IP: 140.113.38.11 On: Thu, 25 Dec 2014 02:06:00

JOURNAL OF APPLIED PHYSICS 115, 083707 (2014)

Experimental and simulation analysis of concave-down resistance curve during electromigration in solder joints

C. K. Lin, Yuan Wei Chang, and Chih Chen[a)]
Department of Materials Science and Engineering, National Chiao Tung University, Hsin-chu 30010, Taiwan

(Received 2 December 2013; accepted 16 February 2014; published online 28 February 2014)

Resistance curves play a crucial role in detecting damage of solder joints during electromigration. In general, resistance increases slowly in the beginning, and then rises abruptly in the very late stage; i.e., the resistance curve behaves concave-up. However, several recent studies have reported concave-down resistance curves in solder joints with no satisfactory explanation for the discrepancy. In this study, electromigration failure mode in Sn2.5Ag solder joints was experimentally investigated. The bump resistance curve exhibited concave-down behavior due to formation of intermetallic compounds (IMCs). In contrast, the curve was concave-up when void formation dominated the failure mechanism. Finite element simulation was carried out to simulate resistance curves due to formation of IMCs and voids, respectively. The simulation results indicate that the main reason causing the concave-down curve is rapid formation of resistive Cu_6Sn_5 IMCs in the current-crowding region, which are 9 times larger than Cu IMCs. Therefore, when Cu reacted with Sn to form Cu_6Sn_5 IMCs, resistance increased abruptly, resulting in the concave-down resistance curve. © *2014 AIP Publishing LLC*. [http://dx.doi.org/10.1063/1.4867048]

I. INTRODUCTION

Flip-chip solder joints have become the most popular packaging technology for high-density input/output (I/O) microelectronic devices.[1] The thickness of the flip-chip solder joints ranges from 70 to 100 μm, and the diameter of the joints is about the same dimension as their thickness. In order to further reduce the dimension of devices, the solder joints have to shrink accordingly. In addition, the required performance of the devices becomes higher and the operating current in each solder joint increases progressively. Hence, electromigration has become one of the most persistent reliability issues in microelectronic devices.[2–7]

A lot of efforts have been devoted to understanding the electromigration behavior.[8–14] Serious current crowding was observed in flip-chip solder joint. Electromigration may induce void formation in solder.[15–17] In addition, electron flow may enhance the dissolution of under bump metallization (UBM), causing extensive formation of intermetallic compounds (IMCs).[18–22] Therefore, Cu columns of about 50 μm thick were adopted as UBMs to relieve the current-crowding effect.[23]

Only a few papers had reported on the electromigration failure mechanism for solder joints with Cu column structures.[23–25] Nah *et al*. found that 50-μm-thick Cu columns can relieve the current-crowding effect in solder joints.[24] Consequently, the electromigration lifetime was enhanced by thick Cu columns.[25]

During electromigration in typical flip-chip solder joints, the resistance of the joints does not increase much during the initial stage of current stressing. The resistance then increases gradually but rises abruptly towards the end of electromigration, thus giving a concave-up resistance curve.[26] However, for electromigration in microbumps with solder thickness less than 20 μm under high current densities, the resistance curve behaves completely different.[27–30] The resistance increases abruptly in the beginning, followed by more gradual increase, thus causing the resistance curve to behave concave-down. Wei *et al*. conducted electromigration tests in microbumps by 9.6×10^4 A/cm^2 at 168 °C and they observed concave-down resistance curves.[27] Lin *et al*. stressed microbumps at 1.23×10^5 A/cm^2 at an ambient temperature of 130 °C and they detected concave-down resistance curves.[28] Similar results were also found in 5 μm-thick-solder microbumps with 30 μm pitch stressed at 10^4–10^5 A/cm^2 at 150 °C.[29] Chen *et al*. also reported a fast initial rise in resistance, then gradually taper-off and reaches a steady state after prolonged stressing in microbumps stressed under 1.0×10^5 A/cm^2 at 140 °C.[30] However, there have been no studies addressing this interesting phenomenon and the discrepancy in results.

This study examined the electromigration in 15-μm SnAg solder joints with 50-μm-thick Cu column UBMs. Concave-down resistance curves were observed experimentally at current stressing of 2.72×10^4 A/cm^2 at 100 °C. Finite element analysis (FEA) was employed to investigate the main reason for the concaved resistance curve. It is found that formation of resistive Cu_6Sn_5 IMCs in the current-crowding region is responsible for the interesting behavior of the resistance curve.

II. EXPERIMENTAL

Lead-free Sn-2.3Ag solder joints were adopted for the electromigration tests. The schematic drawing of the solder joints is shown in Fig. 1(a). The thickness of Cu wiring was 5 μm on the chip side and 27 μm on the FR-5 substrate side. Both traces were 100 μm wide. The dimension of Cu column UBM on the chip side was 50 μm thick. The UBM opening

[a)]Author to whom correspondence should be addressed. Electronic mail: chih@mail.nctu.edu.tw

 © 2014 AIP Publishing LLC

[This article is copyrighted as indicated in the article. Reuse of AIP content is subject to the terms at: http://scitation.aip.org/termsconditions. Downloaded to] IP: 140.113.38.11 On: Thu, 25 Dec 2014 02:06:00

was 140 μm in diameter. The bump height was approximately 15 μm. On the substrate side, the metallization was also Cu with a 140-μm opening. For the as-fabricated sample, the interfacial IMCs were Cu_6Sn_5 on both chip and substrate sides. Figure 1(b) shows the Kelvin bump structures employed to measure individual bump resistance. Some of the solder joints were stressed by 2 A at 100 °C, producing a nominal current density of 2.72×10^4 A/cm^2 on the UBM opening. The real stressing temperature was calibrated using the temperature coefficient of resistivity of the Cu trace on the chip side. The real stressing temperature increased to 176 °C under current stressing due to the Joule heating effect in the solder joints. Some of the joints were stressed at 1.82×10^4 A/cm^2 at 176 °C.

When the bump resistance increased by 5% of the initial bump resistance, current stressing was terminated and cross-sectional observation was performed by a JEOL 6700 scanning electron microscope (SEM). Energy dispersive spectrometer (EDS) was employed to analyze the composition of the solder joint and IMCs. Focused ion beam (FIB) was utilized to observe the microstructures change after current stressing.

III. SIMULATION

To analyze the reason accounting for the concave-down resistance curve, FEA was employed to simulate the changes in resistance due to formation of void and IMCs at various stages. The detailed simulation method has been previously described.[31] To obtain the evolution of the resistance curve for each specimen, 75 models were constructed to simulate the effect of IMC formation at different stages on increase in bump resistance.

IV. RESULTS AND DISCUSSION

Extensive IMC formation was observed after stressing by high current densities. Figure 2(a) shows the microstructure of the as-fabricated bump with binary IMCs of Cu_6Sn_5 formed at the interface of Cu and solder on both chip and substrate sides. Figure 2(b) shows the change in microstructure when bump resistance increases by 5% of its original value after current stressing by 2.72×10^4 A/cm^2 at 176 °C for 366 h. As can be seen, electrons migrated from the bottom-left corner to the upper right corner. The solder joint became a complete Cu_6Sn_5 joint when bump resistance increased by 5% of its initial value. There was no void formation near the electron entrance region. The entire solder layer can react with Cu metallization to form complete IMC joints. Therefore, the change in resistance was mainly attributed to formation of IMCs.

The resistance curve behaves concave-up when voids form and propagate along the interface of solder and UBM during electromigration.[17] Figure 3(a) shows the cross-sectional SEM image of void formation after electromigration at 6.5×10^3 A/cm^2 at 150 °C for 756 h. The corresponding resistance curve is shown in Fig. 3(b). The bump resistance rose slowly in the initial stage of electromigration. As voids propagated along the solder/UBM interface, the resistance

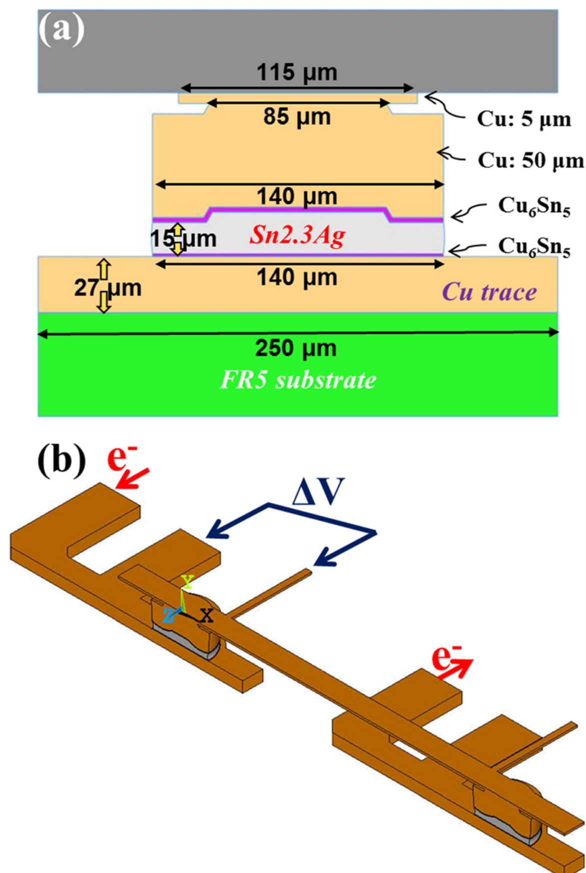

FIG. 1. (a) Schematic structure of solder joint configuration used in this study. (b) Layout for electromigration tests and four-point structure for measuring bump resistance.

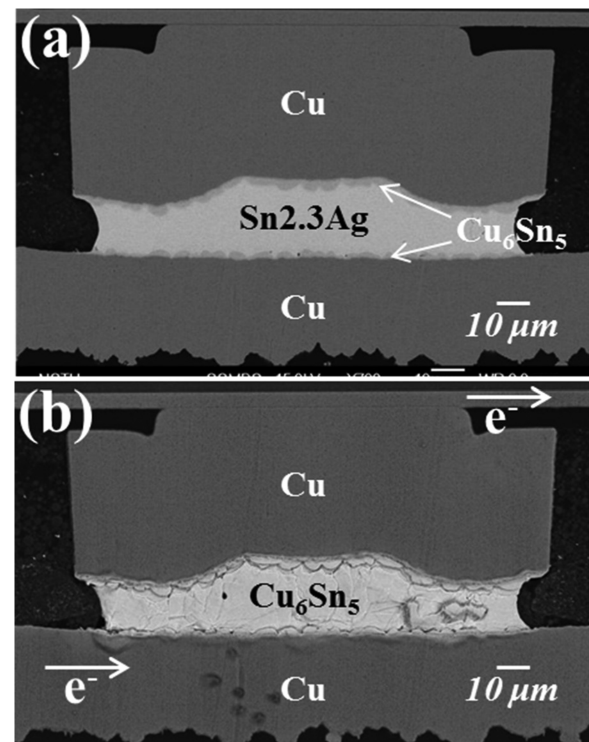

FIG. 2. (a) Cross-sectional SEM image showing the microstructure of an as-fabricated solder bump. (b) The microstructure of solder joints with an upward electron flow after current stressing by 2.72×10^4 A/cm^2 at 176 °C for 366 h. The solder layer was converted into a Cu_6Sn_5 joint.

[This article is copyrighted as indicated in the article. Reuse of AIP content is subject to the terms at: http://scitation.aip.org/termsconditions. Downloaded to] IP: 140.113.38.11 On: Thu, 25 Dec 2014 02:06:00

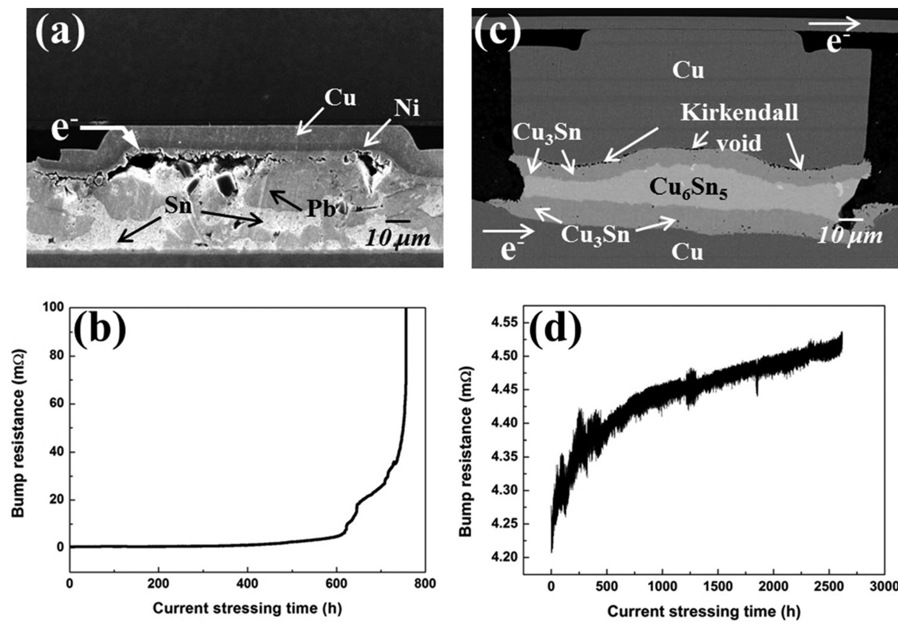

FIG. 3. (a) Cross-sectional SEM image showing electromigration-induced void formation in a solder joint with a downward electron flow after current stressing by 6.50×10^3 A/cm^2 at 150 °C for 756 h. (b) The corresponding curve for bump resistance as a function of stressing time for the joint in (a). (c) Cross-sectional SEM image presenting extensive IMC formation in a solder joint with an upward electron flow after current stressing by 1.82×10^4 A/cm^2 at 156 °C for 2618 h. (d) The corresponding curve for bump resistance as a function of stressing time for the joint in (c).

increased gradually as voids grew. At the final stage, the resistance increased abruptly due to the very small contact opening left.

On the other hand, the resistance curve exhibits a concave-down behavior for solder joints subjected to high-density current stressing. Figure 3(c) presents the cross-sectional SEM image for the solder joint with 15-μm bump height after the electromigration test at 1.82×10^4 A/cm^2 at 156 °C for 2619 h. Extensive IMC formation was found at the current-crowding region. Figure 3(d) illustrates the detected resistance curve, which shows a behavior completely different from that seen in Fig. 3(b). The resistance curve in Fig. 3(d) increased rapidly right after current stressing, followed by a gradual rise in resistance. This behavior was also reported in several previous studies.[27–30]

To investigate the reason behind the different behaviors of the resistance curve, FEA modeling was carried out. The structure of the solder joint was almost identical to the one in Fig. 2(a), in which the solder thickness is 15 μm. Figure 4 presents the constructed model with meshes for a solder joint. The electron flow enters the joint from the bottom-left Cu line and leaves the joint from the upper-right trace. In this model, it is assumed that the solder can react only with the "Cu reaction layer" on the substrate side. The Cu reaction layer was labeled in Fig. 4 and the thickness is 7.5 μm. On the other hand, voids form only in the "void formation layer," as shown in Fig. 4.

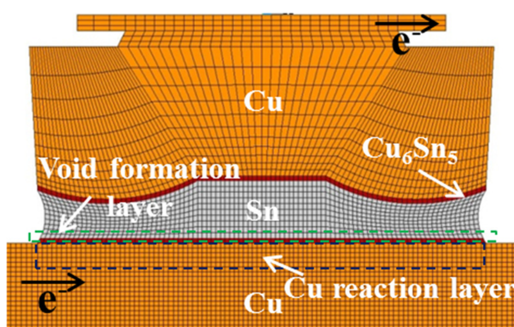

FIG. 4. Schematic meshed model of the constructed solder joint for FEA simulation. The dotted line at the bottom of the Sn layer is the void formation layer. The dotted line on the top of the Cu layer on the substrate side is the Cu reaction layer.

When the resistance increase is caused by void formation only, the resistance exhibits a concave-up behavior. Figures 5(a)–5(e) display the evolution of void when void formation dominates the failure mechanism, showing 0%, 25%, 50%, 75%, and 95% void depletion of the bottom contact opening, respectively. The corresponding evolution of current density is depicted in Figs. 5(f)–5(j). Void formation started from the bottom-left corner of the joint and propagated toward the right-hand side of the joint. Figure 5(k) presents simulated resistance values as a function of void depletion percentage of the bottom contact opening. To obtain this curve, 75 stages were constructed to measure the bump resistance at different void sizes. The behavior of the curve is quite similar to the one in Fig. 3(b). The resistance increased slowly in the early and middle stages, but rose abruptly in the final stage.

However, when the formation of IMCs dominates the failure mechanism, the resistance curve behaves quite differently. The location of IMC formation also has a significant impact on the behavior of the curve. Figure 6(a) presents a cross-sectional for the constructed model before the electromigration-induced IMC formation, in which the electron migrated from the bottom-left corner of the joint to the joint at the upper-right corner. Hence, the current density on the left-hand side of the solder was higher than that on the right-hand side. In this model, it is assumed that the Cu_6Sn_5 IMCs started to grow at the maximum current-density Sn region. As the Sn at this region was consumed to form IMCs, the simulation program chose the remaining Sn region with the highest current density to react with Cu in the "Cu reaction layer" with the highest current density to form Cu_6Sn_5 IMCs. A total of 75 stages were constructed to simulate the resistance curve. Figures 6(b)–6(e) present the evolution of

[This article is copyrighted as indicated in the article. Reuse of AIP content is subject to the terms at: http://scitation.aip.org/termsconditions. Downloaded to] IP: 140.113.38.11 On: Thu, 25 Dec 2014 02:06:00

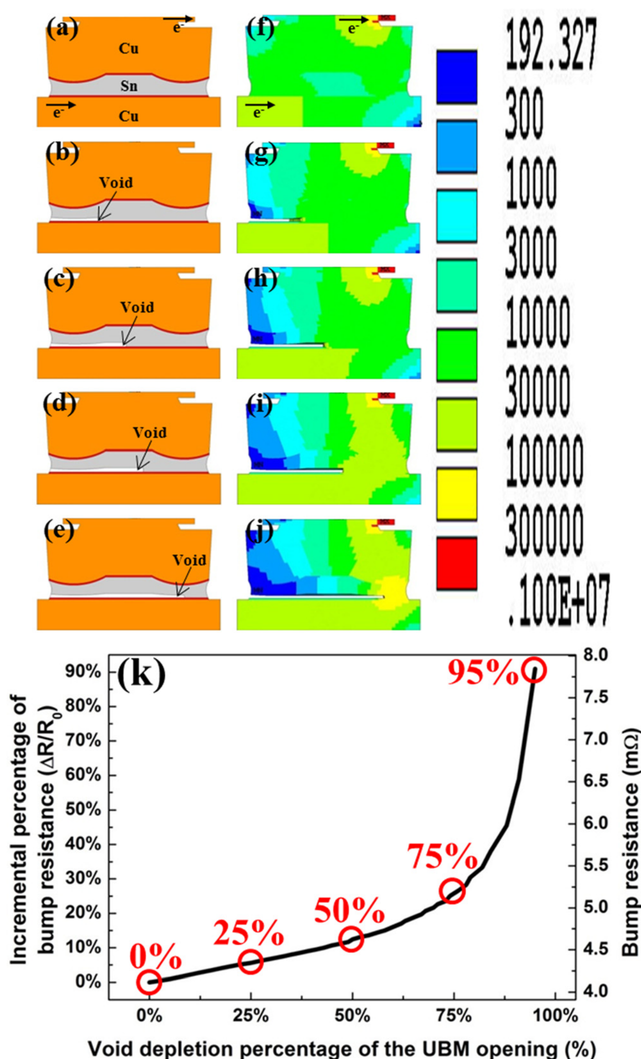

FIG. 5. Simulation of void formation at (a) 0%, (b) 25%, (c) 50%, (d) 75%, and (e) 95% void depletion of the UBM opening, and the corresponding current density distribution in the solder joint at (f) 0%, (g) 25%, (h) 50%, (i) 75%, and (j) 95% void depletion of the UBM opening. (k) The simulated resistance curve as a function of void depletion percentage of the UBM opening.

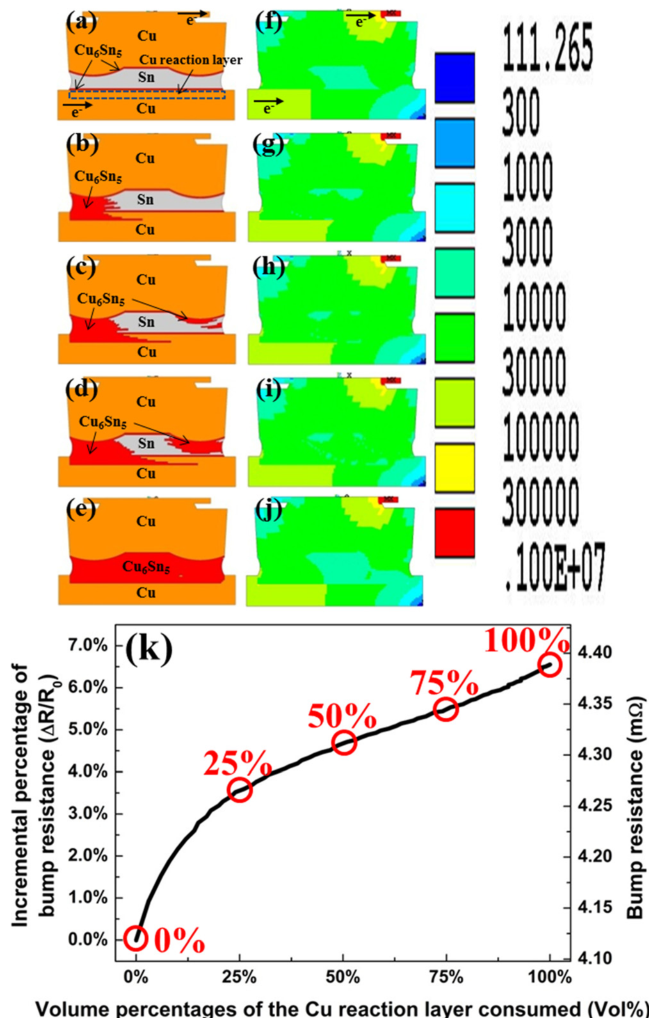

FIG. 6. Simulation of Cu_6Sn_5 IMC formation at (a) 0%, (b) 25%, (c) 50%, (d) 75%, and (e) 100% of the Cu reaction layer consumed, assuming that IMCs started to form at the high current-density region, and the corresponding current density distribution in the solder joint when (f) 0%, (g) 25%, (h) 50%, (i) 75%, and (j) 100% of the Cu reaction layer was consumed. (k) The simulated resistance curve as a function of volume percentages of the Cu reaction layer consumed.

the Cu_6Sn_5 IMC growth at some of the stages. The percentage values represent the consumption ratios of the 7.5-μm "Cu reaction layer" on the substrate side. This Cu region was labeled by the dotted black rectangle in Fig. 6(a). Figures 6(f)–6(j) show the evolution of current-density distribution at different stages. As can be seen, more current stayed drifting in the Cu line on the substrate side when more Cu-Sn IMCs formed at the interface of Cu/solder on the substrate side because Cu-Sn IMCs have higher resistivity than Cu IMCs. However, the difference is not as large as the results shown in Fig. 5. There was still much current passing through the resistive IMC layer. The resistivity of Cu_6Sn_5 IMCs is approximately 9 times larger in magnitude than that of Cu IMCs; hence, the resistance increased significantly when Cu_6Sn_5 IMCs formed. Figure 6(k) presents the evolution of resistance during various stages of IMC formation. The resistance rises abruptly in the initial stage before 25% consumption of the Cu layer, followed by approximately linear increase. The abrupt rise in the initial stage is attributed to the Cu_6Sn_5 formation at the current-crowding region, and most of the Cu there was transformed into resistive Cu_6Sn_5 IMCs. The behavior of the simulated curve in Fig. 6(k) is similar to the experimental curve shown in Fig. 3(d). Therefore, the concave-down behavior is caused by the resistive IMC formation in the current-crowding region.

To examine whether the location of IMC formation would affect the behavior of the resistance curve, more simulation was performed. Figures 7(a)–7(f) present the simulation results when Cu_6Sn_5 grew uniformly on the two solder/Cu interfaces. The simulation curve was illustrated in Fig. 7(g). It is intriguing that the resistance increases linearly with the thickening of the IMC layers. This case may happen when there is no current effect in the solder joint. In addition, when the Cu_6Sn_5 IMCs started to form from the low current-density region, and then grew toward the high current-density region, the resistance curve behaves differently. It is noteworthy to state that this is a fictitious case because the Cu UBM dissolves faster at regions with high

[This article is copyrighted as indicated in the article. Reuse of AIP content is subject to the terms at: http://scitation.aip.org/termsconditions. Downloaded to] IP: 140.113.38.11 On: Thu, 25 Dec 2014 02:06:00

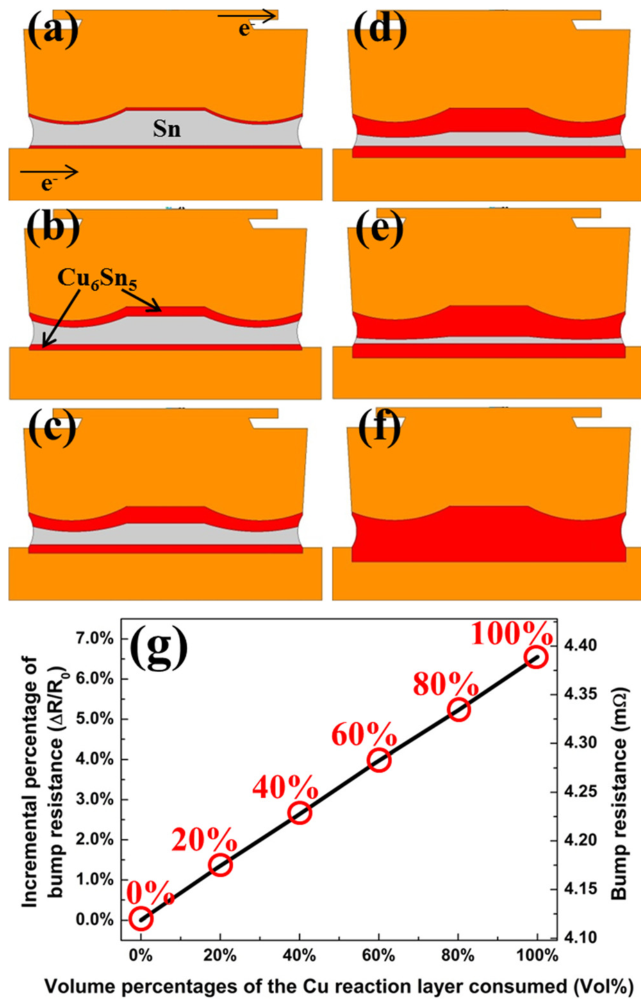

FIG. 7. Simulation of Cu_6Sn_5 IMC formation at (a) 0%, (b) 20%, (c) 40%, (d) 60%, (e) 80%, and (f) 100% of the Cu reaction layer consumed, assuming that IMCs grew uniformly at the two Cu/solder interfaces. (g) The simulated resistance curve as a function of volume percentages of the Cu reaction layer consumed.

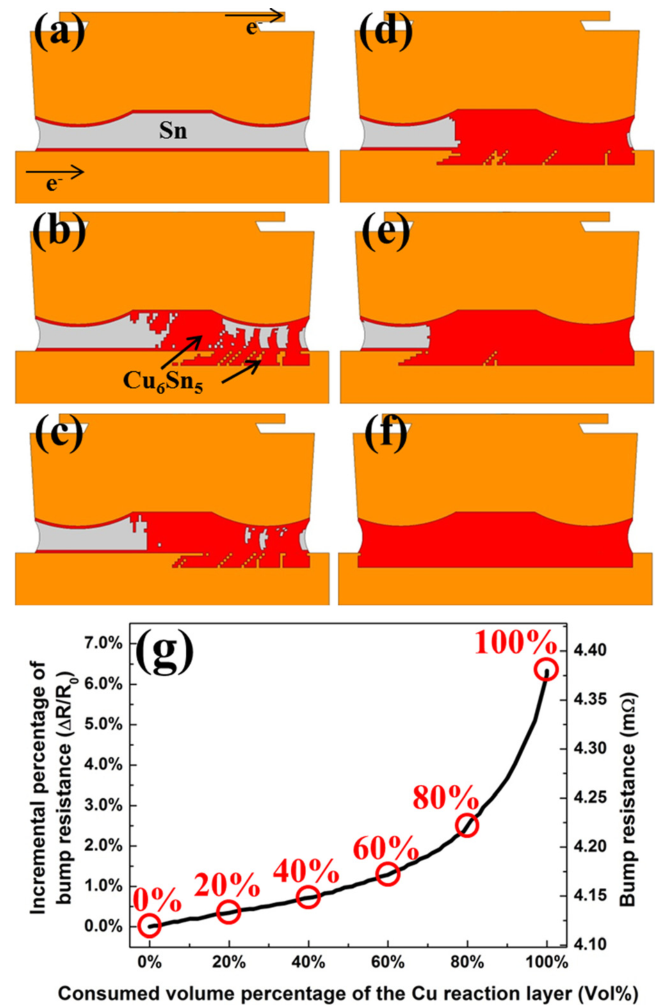

FIG. 8. Simulation of Cu_6Sn_5 IMC formation at (a) 0%, (b) 20%, (c) 40%, (d) 60%, (e) 80%, and (f) 100% of the Cu reaction layer consumed, assuming that IMCs started to form at the low current-density region. (g) The simulated resistance curve as a function of volume percentages of the Cu reaction layer consumed.

current densities than those at low current densities. Figures 8(a)–8(f) show the evolution of IMC growth at various stages. The right-hand side was the low current-density region, whereas the left-hand side was the high current-density region. IMCs started to form in the low current-density region, as illustrated in Fig. 8(b), and then propagated toward the high current-density region. As depicted in Figs. 5(f) and 6(f), the Cu with the lowest current density located at the bottom-right corner of the Cu reaction layer. Thus, Cu started to dissolve there. In addition, the solder with the lowest current density located approximately at the middle-bottom of the joint. Therefore, the Cu-Sn IMCs stared to form there and grew upward to bridge the joint. Then they propagated to the right-hand side of the joint. Once the IMCs formed, they would disturb the distribution of the current density, resulting in the irregular shape of the IMCs. Figure 8(g) presents the simulated resistance curve. Surprisingly, the resistance curve behaves concave-up. This is because when the resistive Cu_6Sn_5 IMCs formed at the low current-density region, only little current passed through the IMCs. Therefore, the resistance did not increase much in the beginning. However, more current passing through the resistive IMCs at later stages resulted in abrupt increase in resistance. Thus, the resistance curve behaves concave-up. It is noted that this case do not happen in real solder joint during electromigration.

It is noteworthy that in order to observe the concave-down resistance curve, the current density should be large enough to trigger IMC formation at the initial stage. In general, the current density should exceed 1×10^4 A/cm^2 and the temperature should be above 130 °C.[30] The stressing conditions for microbumps are usually more stringent than these conditions. Therefore, an abrupt increase in resistance was observed in the literature.[27–30] However, if the current density is small and the temperature is low, then IMC formation does not occur in the beginning. Thus, the resistance curve will not behave concave-down.

V. CONCLUSIONS

Both experimental and simulation approaches were carried out to investigate the resistance curve during electromigration. When void formation dominates the failure

[This article is copyrighted as indicated in the article. Reuse of AIP content is subject to the terms at: http://scitation.aip.org/termsconditions. Downloaded to] IP: 140.113.38.11 On: Thu, 25 Dec 2014 02:06:00

mechanism, the resistance increases very slowly in the beginning and middle stages, followed by an abrupt rise in the final stage. The resistance curve thus behaves concave-up. On the contrary, when IMC formation becomes the dominant failure mechanism at high current densities, the resistance increases rapidly in the initial stage due to formation of resistive IMCs at the current-crowding region, followed by gradual increase in resistance. Therefore, a concave-down resistance curve is observed. In addition, if the IMCs grow uniformly at the Cu/solder interfaces, the resistance increases linearly. This study provides a better understanding on the behavior of resistance curve during current stressing.

ACKNOWLEDGMENTS

The authors gratefully acknowledge the financial support of the National Science Council of the Republic of China (Grant No. NSC 99-2221-E-009-040-MY3).

[1]K. N. Tu, J. Appl. Phys. **94**, 5451 (2003).
[2]C. Chen, H. M. Tong, and K. N. Tu, Annu. Rev. Mater. Sci. **40**, 531 (2010).
[3]C. Y. Liu, K. N. Tu, T. T. Sheng, C. H. Tung, D. R. Frear, and P. Elenius, J. Appl. Phys. **87**, 750 (2000).
[4]Y. C. Chan, A. C. K. So, and J. K. L. Lai, Mater. Sci. Eng., B. **55**, 5 (1998).
[5]H. Gan and K. N. Tu, J. Appl. Phys. **97**, 063514 (2005).
[6]C. Y. Liu, C. Chen, C. N. Liao, and K. N. Tu, Appl. Phys. Lett. **75**, 58 (1999).
[7]S. Brandenburg and S. Yeh, "Electromigration studies of flip-chip solder bump solder joints," in *Proceedings of the Surface Mount International Conference and Exhibition, San Jose* (1998), pp. 337–344.
[8]C. M. Chen and S. W. Chen, J. Electron. Mater. **28**, 902 (1999).
[9]T. Y. Lee, W. J. Choi, K. N. Tu, J. W. Jang, S. M. Kuo, J. K. Lin, D. R. Frear, K. Zeng, and J. K. Kivilahti, J. Mater. Res. **17**, 291 (2002).
[10]T. L. Shao, S. W. Liang, T. C. Lin, and C. Chen, J. Appl. Phys. **98**, 044509 (2005).
[11]M. Ding, G. Wang, B. Chao, P. S. Ho, P. Su, and T. Uehling, J. Appl. Phys. **99**, 094906 (2006).
[12]Y. H. Lin, Y. C. Hu, C. M. Tsai, C. R. Kao, and K. N. Tu, Acta Mater. **53**, 2029 (2005).
[13]C. T. Lin, Y. C. Chuang, S. J. Wang, and C. Y. Liu, Appl. Phys. Lett. **89**, 101906 (2006).
[14]Y. H. Liu and K. L. Lin, J. Mater. Res. **20**, 2184 (2005).
[15]E. C. C. Yeh, W. J. Chos, K. N. Tu, P. Elenius, and H. Balkan, Appl. Phys. Lett. **80**, 580 (2002).
[16]T. L. Shao, Y. H. Chen, S. H. Chiu, and C. Chen, J. Appl. Phys. **96**, 4518 (2004).
[17]Y. W. Chang, T. H. Chiang, and C. Chen, Appl. Phys. Lett. **91**, 132113 (2007).
[18]Y. C. Hu, Y. H. Lin, C. R. Kao, and K. N. Tu, J. Mater. Res. **18**, 2544 (2003).
[19]K. Zeng, R. Stierman, T. C. Chiu, D. Edwards, K. Ano, and K. N. Tu, J. Appl. Phys. **97**, 024508 (2005).
[20]S. H. Chae, X. Zhang, K. H. Lu, H. L. Chao, P. S. Ho, M. Ding, P. Su, T. Uehling, and L. N. Ramanathan, J. Mater. Sci. -Mater. EL. **18**, 247 (2007).
[21]Y. C. Liang, W. A. Tsao, C. Chen, D. J. Yao, A. T. Huang, and Y. S. Lai, J. Appl. Phys. **111**, 043705 (2012).
[22]H. Y. Chen, M. F. Ku, and C. Chen, Adv. Mater. Res. **1**, 83 (2012).
[23]L. Xu, J. K. Han, J. J. Liang, K. N. Tu, and Y. S. Lai, Appl. Phys. Lett. **92**, 262104 (2008).
[24]J. W. Nah, J. O. Suh, K. N. Tu, S. W. Yoon, V. S. Rao, V. Kripesh, and F. Hua, J. Appl. Phys. **100**, 123513 (2006).
[25]Y. S. Lai, Y. T. Chiu, and J. Chen, J. Electron. Mater. **37**, 1624 (2008).
[26]Y. W. Chang, S. W. Liang, and C. Chen, Appl. Phys. Lett. **89**, 032103 (2006).
[27]C. C. Wei, C. H. Yu, C. H. Tung, R. Y. Huang, C. C. Hsieh, C. C. Chiu, H. Y. Hsiao, Y. W. Chang, C. K. Lin, Y. C. Liang, C. Chen, T. C. Yeh, L. C. Lin, and C. H. Yu, "Comparison of the electromigration behaviors between micro-bumps and C4 solder bumps," in *Electronic Components and Technology Conference (ECTC)* (2011), pp. 706–710.
[28]T. H. Lin, R. D. Wang, M. F. Chen, C. C. Chiu, S. Y. Chen, T. C. Yeh, L. C. Lin, S. Y. Hou, J. C. Lin, K. H. Chen, S. P. Jeng, and C. H. Yu, "Electromigration study of micro bumps at Si/Si interface in 3DIC package for 28nm technology and beyond," in *Electronic Components and Technology Conference (ECTC)* (2011), pp. 346–350.
[29]Y. M. Lin, C. J. Zhan, J. Y. Juang, J. H. Lau, T. H. Chen, R. Lo, M. Kao, T. Tian, and K. N. Tu "Electromigration in Ni/Sn Intermetallic Micro Bump Joint for 3D IC Chip Stacking," in *Electronic Components and Technology Conference (ECTC)* (2011), pp. 351–357.
[30]H. Y. Chen, D. Y. Shih, C. C. Wei, C. H. Tung, Y. L. Hsiao, C. H. Yu, Y. C. Liang, and C. Chen, "Generic rules to achieve bump electromigration immortality for 3D IC integration," in *Electronic Components and Technology Conference (ECTC)* (2013), pp. 49–57.
[31]S. W. Liang, Y. W. Chang, and C. Chen, Appl. Phys. Lett. **88**, 172108 (2006).

[This article is copyrighted as indicated in the article. Reuse of AIP content is subject to the terms at: http://scitation.aip.org/termsconditions. Downloaded to] IP: 140.113.38.11 On: Thu, 25 Dec 2014 02:06:00